Supplement for

**A new parameterization scheme of the real part of the ambient aerosols refractive index**

Gang Zhao[1], Tianyi Tan[2], Weilun Zhao[1], Song Guo[2], Ping Tian[3], Chunsheng Zhao[1]

1 Department of Atmospheric and Oceanic Sciences, School of Physics, Peking University, Beijing, China

2 State Key Joint Laboratory of Environmental Simulation and Pollution Control, College of Environmental Sciences and Engineering, Peking University, Beijing 100871, China

3 Beijing Key Laboratory of Cloud, Precipitation and Atmospheric Water Resources, Beijing 100089, China

## 1 Measurement Site

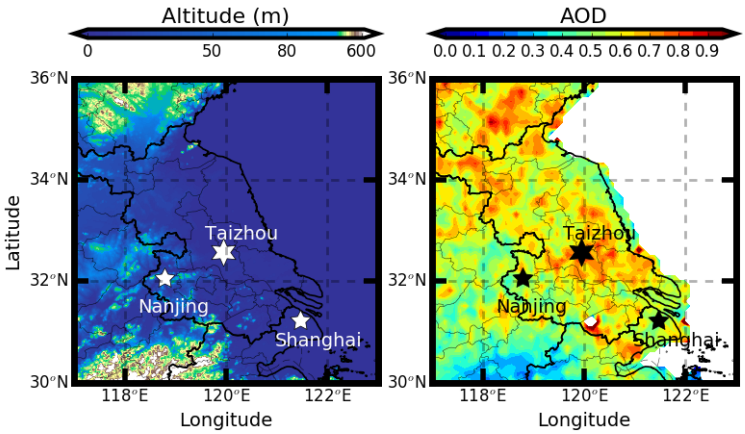


**Figure S1:** Measurement site of Taizhou (marked with stars). Filled colors represent (a) the topography of the Jianghuai Plain. (b) the average aerosol optical depth at 550nm during the year of 2017 from Moderate Resolution Imaging Spectroradiometer onboard satellite Aqua.

## 2 Instrument setup

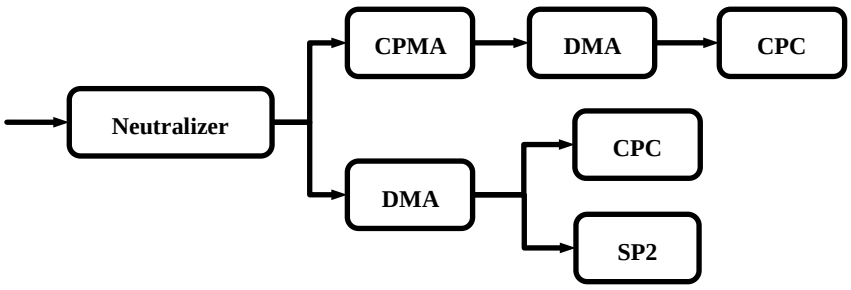


**Figure S2.** Schematic of the instrument setup.

## 3. Calibration of the SP2.

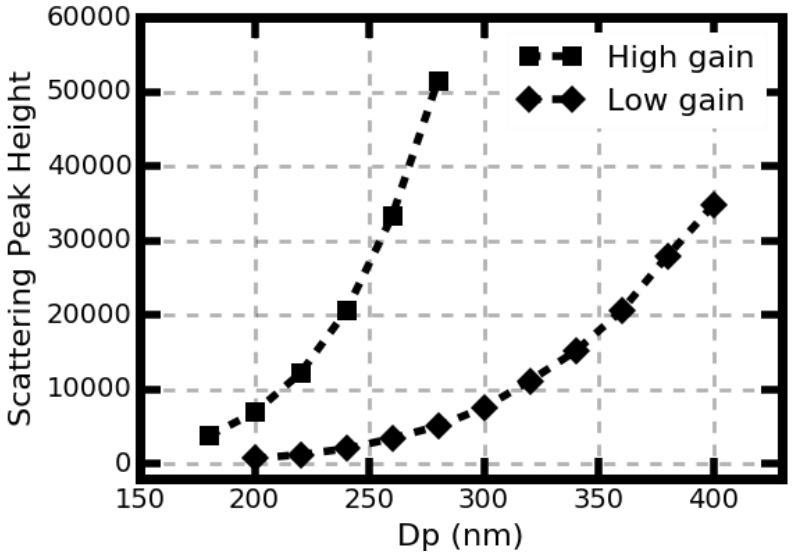


**Figure S3.** The calibrated relationship between the scattering peak height and the ammonia sulfate diameter for both the scattering high gain channel and the scattering low gain channel.

## 4 Overview of the measurement

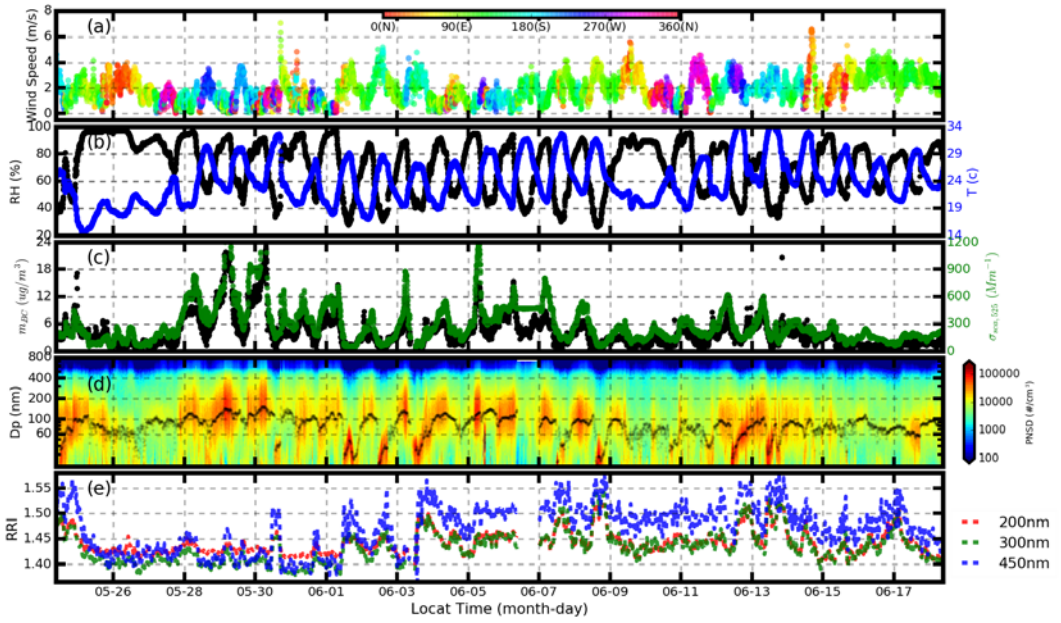


**Figure S4.** The measured time series of the (a) wind speed, (b) RH (black line), temperature (blue line), (c) BC mass concentrations (black line), scattering coefficient at 525 nm (green line), (d) aerosols PNSD (filled color), aerosol median Dp of the corresponding PNSD (black dotted line), (e) aerosol RRI at 200nm (red line), aerosol RRI at 300nm (green line) and aerosol RRI at 450nm (blue line). The filled color in (a) represent the wind direction.

## 5 The daily variation of the temperature, RH, BC mass concentrations and scattering coefficient.

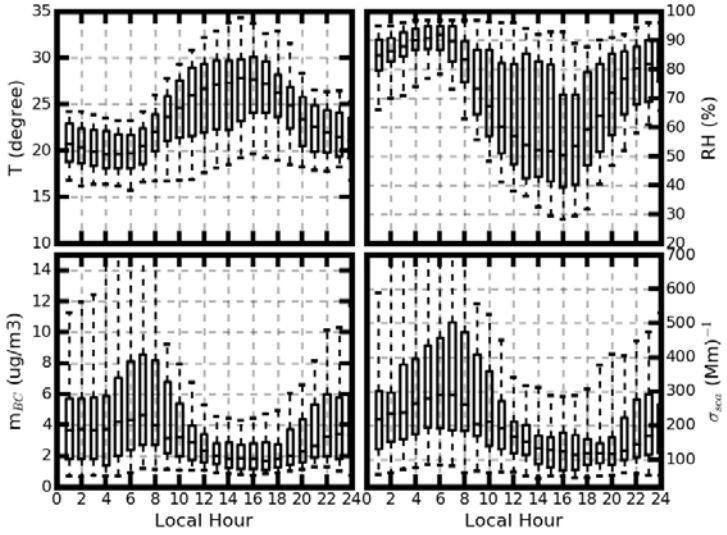


**Figure S5.** Daily variation of the measured (a) temperature, (b) RH, (c) BC mass concentrations and (d) aerosol scattering coefficient.

## 6 The daily variation and probability distribution of the $\rho_{eff}$

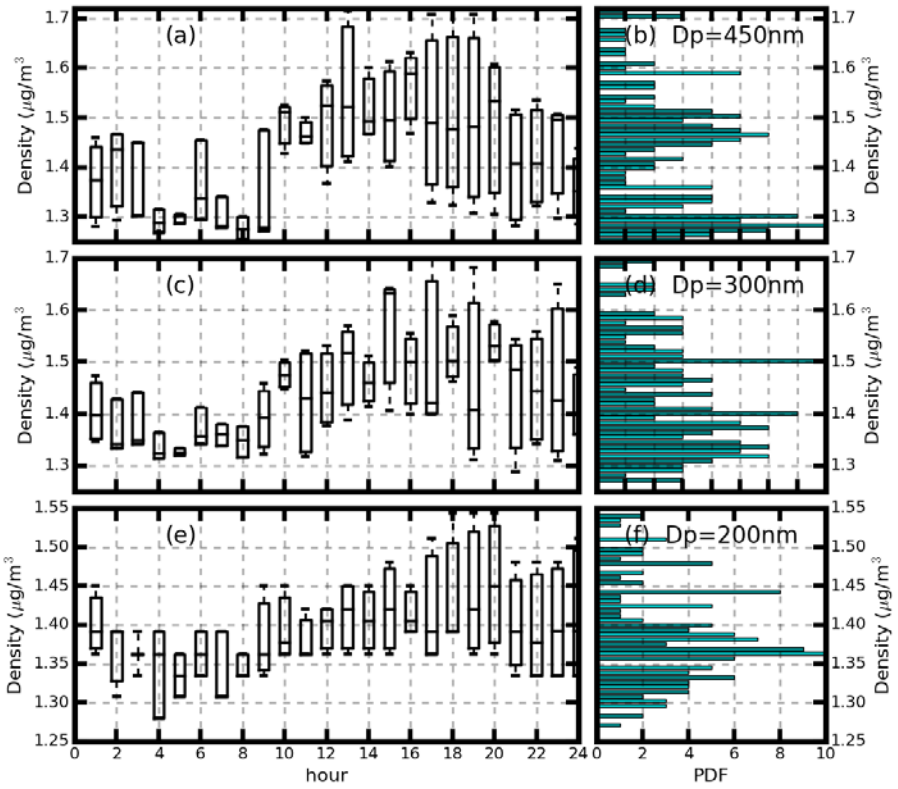


**Figure. S6.** Daily variations of the $\rho_{eff}$ (a), (c) (e), and the probability distribution of the measured $\rho_{eff}$ (b), (d) (f) for the (a), (b) 200 nm, (c), (d) 300 nm, and (e), (f) 450nm aerosol.

## 7. Comparison the measured RRI Aerosol Components

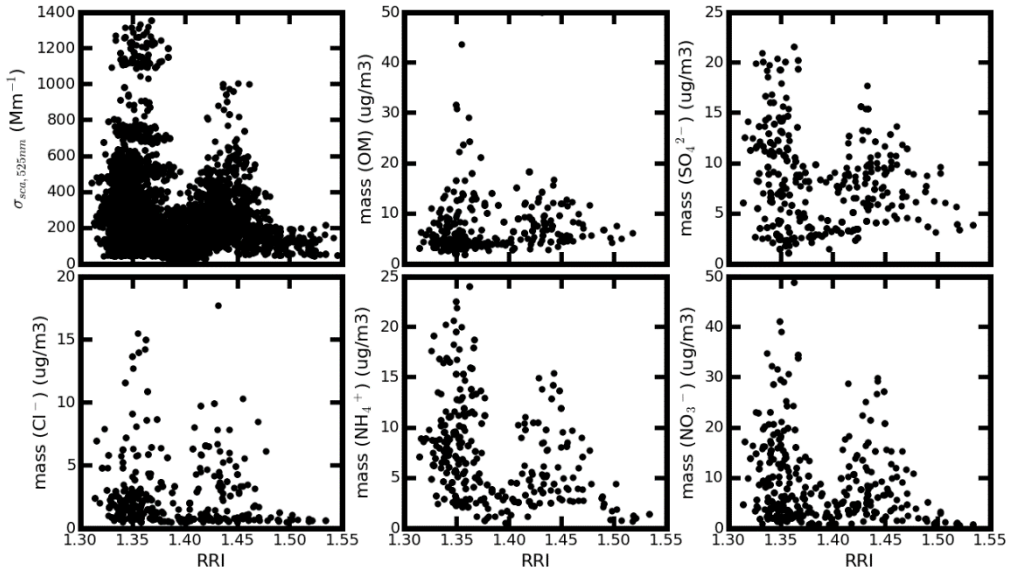


**Figure S7.** Comparison the measured RRI at 300nm with the measured (a) $\sigma_{sca}$ at 525nm, mass concentrations of (b) OM, (c) $SO_4^{2-}$, (d) $Cl^-$, (e) $NH_4^+$ and (f) $NO_3^-$.

## 8 Comparison between the calculated and measured RRI.

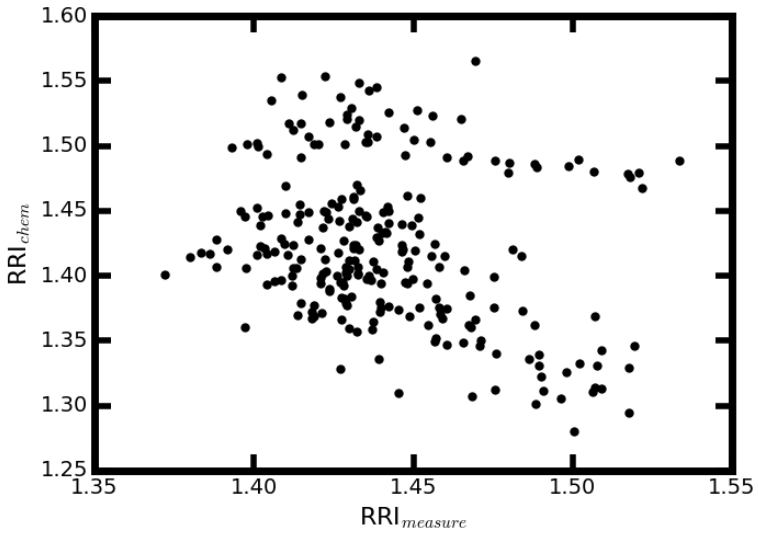


**Figure S8.** Comparison between the calculated RRI ($RRI_{chem}$) using the method of Stelson (1990) and measured RRI ($RRI_{measure}$). The filled color represent the Julian day of the year 2018.

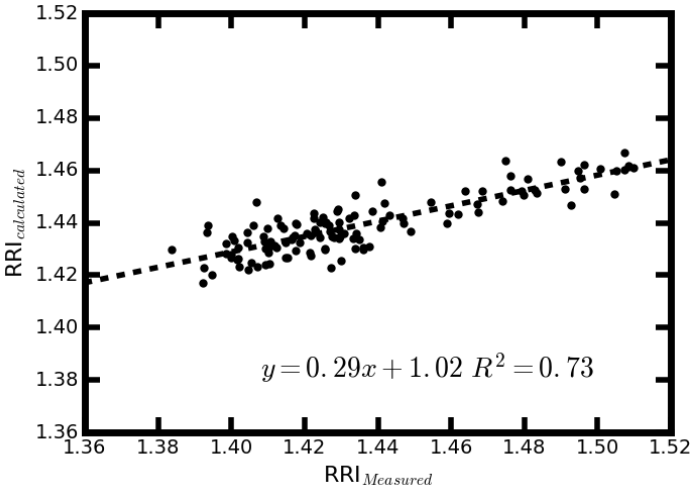


**Figure S9.** Comparison between the calculated RRI ($RRI_{chem}$) using the method of Liu and Daum (2008) and measured RRI ($RRI_{measure}$). The filled color represent the Julian day of the year 2018.

Liu, Y., and Daum, P. H.: Relationship of refractive index to mass density and self-consistency of mixing rules for multicomponent mixtures like ambient aerosols, Journal of Aerosol Science, 39, 974-986, 10.1016/j.jaerosci.2008.06.006, 2008.

Stelson, A. W.: Urban aerosol refractive index prediction by partial molar refraction approach, Environ.sci.technol, 24:11, 1676-1679, 1990.